

A Proximity-based Approach for Dynamically Matching Industrial Assets and Their Operators Using Low-Power IoT Devices

Silvano Cortesi[✉], *Graduate Student Member, IEEE*, Michele Crabolu[✉], *Prodromos-Vasileios Mekikis[✉]*, Giovanni Bellusci[✉], Christian Vogt[✉], *Member, IEEE* and Michele Magno[✉], *Senior Member, IEEE*

Abstract—Asset tracking solutions have proven their significance in industrial contexts, as evidenced by their successful commercialization (e.g., Hilti On!Track). However, a seamless solution for matching assets with their users, such as operators of construction power tools, is still missing. By enabling asset-user matching, organizations gain valuable insights that can be used to optimize user health and safety, asset utilization, and maintenance. This paper introduces a novel approach to address this gap by leveraging existing Bluetooth Low Energy (BLE)-enabled low-power Internet of Things (IoT) devices. The proposed framework comprises the following components: i) a wearable device, ii) an IoT device attached to or embedded in the assets, iii) an algorithm to estimate the distance between assets and operators by exploiting simple received signal strength indicator (RSSI) measurements via an Extended Kalman Filter (EKF), and iv) a cloud-based algorithm that collects all estimated distances to derive the correct asset-operator matching. The effectiveness of the proposed system has been validated through indoor and outdoor experiments in a construction setting for identifying the operator of a power tool. A physical prototype was developed to evaluate the algorithms in a realistic setup. The results demonstrated a median accuracy of 0.49 m in estimating the distance between assets and users, and up to 98.6% in correctly matching users with their assets.

Index Terms—*iot, edge computing, sensor network, signal processing, cloud computation, embedded systems, low-power, bluetooth low energy, tracking*

I. INTRODUCTION

In recent years, the proliferation of connected devices has not only changed everyday life, but has also transformed the industrial sector [1], [2]. At the center of this is the broad availability of Internet of Things (IoT), which is establishing into smart homes, smart cities, and smart manufacturing, among others [3], [4]. Nevertheless, the construction industry still lags behind other industries regarding digitalization and efficiency [5], [6]. Due to their inherent complexity involving different activities, stakeholders, and dynamic environments, construction projects are prone to risks such as delays, cost overruns, quality defects, and accidents [7].

Asset-tracking solutions have gained prominence in industrial contexts to tackle some of these issues, as evidenced

(Corresponding author: Silvano Cortesi, silvano.cortesi@pbl.ee.ethz.ch.)

Silvano Cortesi, Christian Vogt and Michele Magno are with the Center for Project-Based Learning, ETH Zürich, 8092 Zürich, Switzerland (e-mail: firstname.lastname@pbl.ee.ethz.ch)

Michele Crabolu, Prodromos-Vasileios Mekikis and Giovanni Bellusci are with Hilti AG, 9494 Schaan, Liechtenstein (e-mail: firstname.lastname@hilti.com)

by their successful commercialization [8]. Yet, one significant gap is the lack of precise tracking of which operator uses which asset [9]. Addressing this gap provides valuable insights that can be exploited to improve efficiency and safety across various industries. Examples include:

- **Healthcare Settings:** Tracking which medical professional uses a specific device (e.g., mobile X-ray or ultrasound machines), improves patient safety by ensuring only authorized personnel operate critical equipment, and facilitates timely maintenance [10], [11].
- **Manufacturing Environments:** Monitoring operators and machines (e.g., welding equipment, forklifts) enhances maintenance scheduling and detects the need for retraining, reducing breakdowns and downtime, while optimizing operational costs [12].
- **Construction Projects:** Operator-to-asset tracking on construction sites offers insights into tool usage, productivity, and equipment management. This helps to identify misuse, reduce wear and tear, and ensure compliance with safety regulations [13, p. 195].

By knowing the right operator of a specific asset and the duration of the performed activity, it is possible to automatically generate asset-usage reports, check operators' tools safety training, and open a pipeline to allow easier digitalization of job sites. In turn, this additional granularity can further improve the existing asset management approaches [14], [15].

In the pursuit of achieving asset-operator matching, several technical approaches can be explored. Among these, biometric systems integrated into assets, such as fingerprint readers on power tools, could be considered. Additionally, complex real-time location systems (RTLS) deployed within job sites offer precise tracking capabilities for both users and assets [16]. However, it is essential to acknowledge that these approaches face practical challenges when applied in dynamic industrial environments, particularly within the construction sector. The inherent complexities, high power consumption, and associated costs render them less feasible for widespread adoption.

In the context of this paper, a novel approach for asset-operator matching is introduced. The fundamental premise underlying this approach is that the operator of a handheld asset must be the one nearest to the asset when it is active. Therefore, to pursue this idea, the following have to be monitored:

- the distance between users and active assets, and

- the real-time status of the asset. Specifically, whether it is active, e.g., in the case of a power tool, if its motor is running. This distinction is crucial for focusing the analysis on only the active assets.

In implementing this novel approach, it is crucial to recognize that pinpointing the exact absolute distance between a user and an asset is not the primary objective. The essence of the method lies in accurately identifying the nearest operator to an active asset. This means that absolute accuracy in measuring the distance between the asset and the operator is not necessary. What is important is the relative distances between operators and the asset. For example, if Operator *A* is estimated to be at a distance of 2 m and Operator *B* at 4 m from asset #1, despite their actual distances being 1 m and 3 m respectively, the system effectively discerns that Operator *A* is the nearest.

Given that most of the already deployed asset management systems are Bluetooth Low Energy (BLE)-based (e.g., Hilti On!Track) and that BLE received signal strength indicator (RSSI) is a function of the distance, the proximity of the user to the asset can be estimated. However, raw RSSI values are affected by various phenomena, e.g., multi-path effect, leading to inaccurate measurements. To address this challenge, Bayesian filters can be employed. These filters leverage a physical model to exploit all available information and yield a more precise distance estimation [17].

Moreover, asset management IoT devices are generally equipped with at least an accelerometer [18]–[21]. This capability can be utilized to monitor the activity status of the asset, allowing a focus solely on active assets. In our use-case it is assumed that no more than 15 active assets and operators are within BLE range to each other. Leveraging these insights, the contributions of this paper are the following:

- Novel approach: the proposed method is based on the insight that the operator of a handheld asset must be nearest to the asset when it is active. Each operator wears a wearable device that supports BLE and Long-Term Evolution Machine Type Communication (LTE-M) connectivity. The asset is retrofitted with a BLE-based tracking device equipped with an accelerometer. This device periodically broadcasts a message containing information about the asset's activity status estimated with a TinyML algorithm. The wearable receives this message and, if the asset is active, calculates the distance. All user-asset distances are sent to the cloud, where another algorithm sorts and estimates the nearest user to the active asset, assigning them as the asset's user.
- Accurate and energy efficient asset-user distance estimation at the edge: The proposed approach optimizes power consumption across all components. To achieve this, the study explores the possibility to enhance the accuracy of distance estimations from RSSI measurements applying Bayesian filters on ultra-low power asset management IoT devices and wearable devices.
- Real-world validation: The algorithms have been ported on previous developed hardware prototypes, i.e., SMART-TAG [18] and ECOTRACK [22], and tested in a realistic

setup. The system was validated through extensive indoor and outdoor experiments in real construction settings, demonstrating its practical applicability.

The rest of the paper is organized as follows: Section II reviews the state-of-the-art in asset-tracking and wireless distance estimation. Section III presents the high-level system architecture, and Section IV gives an in-depth view of the applied algorithms. Section V describes the experimental setup and the experiments, while Section VI reports and discusses the results. Finally, Section VII concludes the paper and outlines future work.

II. RELATED WORKS

Tracking assets in industrial environments, including construction sites, is nothing new. As early as 2005, Goodrum et al. [23] presented a radio frequency identification (RFID)-based system in which active RFID tags are integrated into power tools to track them. The aim was to find lost tools. In an experimental evaluation, the tools could be found with a personal digital assistant (PDA) up to a distance of 10.5 m, depending on the environment. A similar approach was taken by Goedert et al. [24], whereby utilization tracking was carried out by recognizing which power tools were still in the depot. An RFID-equipped cabinet was able to determine with an accuracy of up to 98% whether a tool is lying in the cabinet or is currently in use. Kwon et al. [25] developed a ultra-wideband (UWB)-based RTLS in 2021 to track tools across the entire construction site with an accuracy of up to 13.3 mm.

The systems presented above are either limited in terms of only detecting whether an asset is currently in use or not, or requiring a widespread anchor setup to ensure accurate localization across the entire industrial environment. The goal of this paper is different: we try to find out when an asset is used, and in particular by which operator, without an RTLS infrastructure, such that the setup effort and costs are minimized. In order to achieve such a system, the first step is to recognize the distance between users and assets with simple IoT devices.

The most common methods for distance measurement using radio frequency are based on RFID, RSSI, time of flight (ToF), or multi-carrier phase-difference (MCPD) [26]. While RFID is limited in range [23], ToF requires a high bandwidth to detect precisely line-of-sight (LOS), requiring a dedicated transmission technology like UWB. MCPD-based ranging requires the bidirectional exchange of multiple messages, thus consuming significantly more power when compared to RSSI-based approaches [27]–[29].

RSSI-based approaches are based on the correlation between the received signal strength and the transmission distance [30]. The decrease of the signal strength can be modeled as logarithmic function of the distance, as shown in Eq. (1) [31]:

$$RSSI(x) = RSSI(x_0) - 10n \cdot \log_{10} \left(\frac{x}{x_0} \right) \quad (1)$$

RSSI-based distance measurements are widely used due to the availability in most radio frontends [32]. Furthermore,

they require only unidirectional transmission, which reduces power consumption at the transmitter end. The widespread use of BLE system-on-chips (SoCs) in modern smartwatches, smartphones, and more makes them an ideal candidate for various IoT applications, including localization. During the COVID pandemic, it was widely utilized to monitor social distance and to keep track of spreading paths by exploiting RSSI measurements [33]–[35] – a use case very similar to ours.

Although the theoretical equation suggests a strong relationship between RSSI and distance, it does not account for all physical aspects in practice. Due to the following factors: *i*) inaccurate measurements [36], *ii*) improper antenna matching [37], *iii*) multipath fading and reflections [38], *iv*) antenna directivity [37], and *v*) attenuations due to obstructed line of sight [39], the relationship between distance and RSSI is highly complex. As the distance increases, the impact of these errors becomes more significant, resulting in lower accuracy compared to methods based on ToF or MCPD. Consequently, the distance from a received signal power can only be predicted to a limited extent.

More accurate modeling of the path-loss that accounts for all factors in different industrial environments is complex, with no single model suitable for universal use [40, p. 27ff]. Despite the many sources of errors, various algorithms have been explored to optimize the accuracy of range measurements based on RSSI using BLE [17], [41]–[43], providing more reliable distance estimation.

Mackey et al. [17] developed a mobile application that uses three Bayesian filtering techniques to process the RSSI measurements received from BLE beacons and estimate the distance between the beacon and the receiver. They focused on the following Bayesian filters: *i*) a Kalman Filter (KF), which assumes a linear model with white and Gaussian noise; *ii*) a Particle Filter (PF), which uses a set of consecutive samples to represent the posterior distribution; and *iii*) a non parametric information (NI) filter, which uses a kernel density estimator to approximate the posterior distribution. The paper reported that with Bayesian filters, the distance estimation accuracy can be improved by up to 39% compared to the moving average when the beacon and the receiver are within 3 m. In a large room, the PF showed the highest improvement of 39% on average, the KF showed an improvement of 25.6%, and the NI by 23.25%. In a small room, the performance of the filters was closer together, with the PF improving by 31% on average, the NI by 30%, and the KF by 28%. Finally, the authors attribute the marginal superiority of the PF over the KF to its non-parametric approximation of the system, which fits the path-loss model better. Furthermore, they state that the runtime of the beacons is up to 21.4 months (Estimote), without providing the exact size of the battery. Due to the higher computational costs of the PF [45] and NI filter compared to the KF, while there is only a marginal difference between the filters, especially in small spaces, our system is based on the Extended Kalman Filter (EKF).

Debnath et al. [44] improved the RSSI-based ranging using a KF followed by a random forest (RF) model with 100 decision trees. The measurements of each BLE advertisement

channel are thereby processed individually before the results are combined by averaging. The experimental evaluation at static measurement positions from 0.5 m to 8.0 m showed an average accuracy of 0.31 m. The computations are performed on a personal computer (PC).

Lee et al. [41] proposed an EKF for enhancing the deteriorated RSSI-based position estimation caused by noise, motion, and fading. In contrast to our approach, fixed BLE anchors and a two-dimensional motion model are used, and the computation is performed on a server. The EKF handles the nonlinearities and uncertainties of both the motion and measurement models. Due to its filter characteristics, it provides a more accurate estimate of the smartphone’s position than trilateration using raw RSSI signals. Experimental measurements have been conducted in an indoor environment using static measurement positions. Their method achieved a localization accuracy of 0.26 m and 0.28 m in x- and y-coordinates over 100 measurements in a 12 m × 11 m room.

In order to further increase the accuracy of distance estimation based on RSSI, Al Qathrady and Helmy [42] integrated the RSSI and knowledge of the BLE TX power level into several parametric and machine learning (ML) models running on a connected PC. The study was conducted based on 1.8 million indoor recordings from static positions at distances between 0.5 m and 22 m. With the integration of the TX power level, they reduced the mean average estimation error by up to 46% compared to their model without TX power level integration. The final precision of the distance estimation was 0.5 m.

Gómez-de-Gabriel et al. [43] deployed BLE beacons in risky areas where a lifeline connected to a harness is needed to monitor the proper usage of harnesses on construction sites. Having an additional beacon on the lifeline itself and a receiver on the harness, they try to estimate whether workers are connected to the lifeline or not in risky areas. Their distance estimation approach is based on an EKF filter running on an ESP32 microcontroller (MCU). The system state model used for the EKF is a *no-motion* motion model [46] where state transitions (i.e., worker movement) are modeled as Gaussian stochastic perturbations. The model is based on the assumption of a maximum worker speed of $0.5 \frac{m}{s}$ with a probability of 95%. Their evaluation in a dynamic setup shows a distance estimation accuracy of ≈ 1 m.

Our approach results in slightly worse accuracies when compared to more sophisticated algorithms such as NI or RF, as shown in Table I. However, due to the limited computational and energy resources and the requirement to run in real-time, this represents the trade-off taken to perform the calculation on an MCU instead of a computer or server. Furthermore, our measurement is in a dynamic setup and not at predefined static distances.

III. SYSTEM ARCHITECTURE

The proposed system consists of three parts (Fig. 1): A sensor tag, a wearable device (worn as a badge), and a centralized server. The sensor tag is a smart BLE node with an activity detection feature used to identify the assets. It advertises the

TABLE I
COMPARISON OF STATE-OF-THE-ART APPROACHES TO IMPROVE BLE-BASED RSSI LOCALIZATION

	IOT'20 [17]	IPIN'23 [44]	MIS'16 [41]	MSWIM'17 [42]	MEAS'19 [43]	This work
Algorithm	KF, NI, PF	KF+RF	EKF	diff. ML	EKF	EKF
Measurement scheme	static	static	static	static	dynamic	dynamic
Localization setup	ranging	ranging	6 anchors	ranging	ranging	ranging
Processing unit	smartphone	PC	server	PC	ESP32	nRF52833
Measured range	0.5 m – 3.0 m	1.0 m – 8.0 m	12 m × 11 m	0.5 m–22 m	0.0 m–7.0 m	0.0 m–6.0 m
Accuracy	0.27 m (PF)	0.31 m	0.26 m × 0.28 m	0.50 m	≈ 1.00 m	0.49 m
Deployment effort	medium	medium	high	medium	low	low

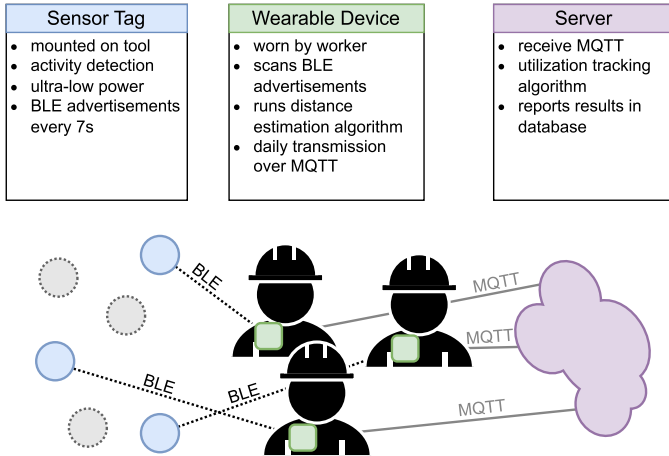


Fig. 1. Overview of the three parts of the system: sensor tags mounted on inactive assets (gray), sensor tags mounted on active assets (blue), wearable devices close to the active sensor tags (green) and a centralized server (violet).

asset's current status every seven seconds, reporting whether it is being used or not. The key factor here is that the tag is characterized by ultra-low power consumption, ensuring a lifetime of multiple years in battery-powered mode when it is retrofitted onto existing tools.

The wearable device, carried by each user and supporting BLE and cellular connectivity, scans for BLE advertisements of such a sensor tag and records its RSSI. In the proposed system architecture, the wearable operates as an edge device, pre-processing the real-time distance measurements to the individual tags and transmitting the aggregated data to a server.

The resulting high variance of the RSSI values can be filtered to remove noise and minimize the deviation from the theoretical path-loss equation proposed by [17], [41]–[43] and discussed in Section II.

Two strategies can be considered for the distance estimation: the first strategy involves transmitting all raw data to the server, where ML-enhanced processing techniques such as deep learning (DL), NI, or RF could provide a more accurate distance estimation. However, this approach requires a considerable amount of data to be transferred from the wearable device to the server.

This high data transmission demand would significantly limit the lifetime of the battery-powered device due to the high power consumption required for data transmission (as shown in Table III), and would also raise transmission costs.

The second option is to exploit the wearables' computing capabilities for estimating the distance between assets and users. As a result, the transmission size can be significantly restricted and kept constant, regardless of the session duration of the asset usage.

To fully benefit from the energy savings of the reduced amount of transmitted data, the computational expenses for distance calculation on the wearable device must be kept low. To achieve this, a 1-state EKF algorithm was selected in this work, which offers good performance as demonstrated in previous studies [41], [43], and requires low computational effort.

Finally, using its cellular interface, the wearable device transmits the estimated distances for each active period of an asset to a centralized server once per day.

After the new distance data arrives from the wearable devices, it is written to a database by the server. The data are sorted by time and organized in sessions. Each of these sessions groups an active period of an asset with the distance data of the users. In solving an optimization problem, the relation between an active asset and its correct user is estimated. The results are then made available to the end user in a dashboard.

IV. ALGORITHMS

The main challenge of the algorithm running on the wearable devices lies in achieving an accurate real-time distance estimation between the sensor tags attached to individual assets and the wearable badge. Due to these devices' limited computation and energy resources, computationally lightweight and energy-efficient algorithms are needed. Furthermore, the distance estimations must be accurate in the face of environmental noise and measurement uncertainties inherently given by the RSSI recordings.

Simultaneously, the asset-user tracking algorithm, which operates on distance measurements aggregated from multiple wearables on a central server, faces its own challenges. While it benefits from greater computational resources compared to wearable devices, it must effectively handle the dynamic nature of tool usage scenarios, where multiple users may interact with each other and the various assets concurrently.

The proposed system to assign assets to their users consists, therefore, of two algorithms:

- A distance estimation algorithm optimized and evaluated on the low-power wearable device.

- An asset-user tracking algorithm, based on an optimization problem, evaluating the distance measurements of all badges and assigning the most probable matching of tags and badges together with a probability classifier, yielding the trust level 'SURE' or 'UNSURE'.

A. Distance Estimation

The state variable of the dynamic system that is attempted to be estimated is the distance x between the tag and the badge. The model is based on the assumption that the distance between the user and the used assets is virtually constant, with random variations around this distance. Specifically, the relative movement between assets and operators can be modeled as random noise; therefore, a *no-motion* motion model [46, p. 169ff] was used. In this model, the state evolution of the kinematic equation consists of propagating the state (i.e. the distance) from the last step without changes; the movement between the operators and assets is modeled as a zero-mean Gaussian stochastic perturbation w_k as in Eq. (3):

$$x_k = x_{k-1} + w_k, \quad w_k \sim \mathcal{N}(0, Q_k) \quad (2)$$

where the process noise covariance Q_k is chosen as

$$Q_k = \frac{v_{max}^2}{\mathcal{X}_{1,c}^2} = 0.1275 \frac{\text{m}^2}{\text{s}^2} \quad (3)$$

with v_{max} the expected maximum relative velocity of the operators with respect to the assets ($0.7 \frac{\text{m}}{\text{s}}$) in 95% of all times ($c = 0.05$) and $\mathcal{X}_{1,c}^2$ the support value of a Chi-squared distribution marking the beginning of an upper tail with area c and 1 degree of freedom.

The observation model is defined in Eq. (4) and follows the path-loss model, with the observation variable z representing the RSSI measurement.

$$z_k = h(x_k) + v_k, \quad v_k \sim \mathcal{N}(0, R_k) \quad (4)$$

$$h(x) = \text{RSSI}(x_0) - 10n \cdot \log_{10} \left(\frac{x}{x_0} \right) \quad (5)$$

The measurement noise covariance R_k in Eq. (6) was evaluated experimentally using all measurement values in Fig. 3.

$$R_k = \sigma^2 = 43.53 \quad (6)$$

The EKF is then composed of two steps, the prediction and the update step, as in [47, p. 310ff], with

$$H_k = \frac{\partial h}{\partial x} \Big|_{\hat{x}_{k|k-1}} = \frac{-10n}{\log(10) \cdot \hat{x}_{k|k-1}}$$

Due to the high variance of the RSSI measurements and the non-linearity of the measurement model, the choice of the initial value can severely impact the filter's evolution and is, therefore, crucial [48].

The initial state estimation was, therefore, based on the path-loss model but restricted to realistic distances:

$$\hat{x}_{0|0} = \max(\min(h^{-1}(\text{RSSI}), 20 \text{ m}), 0.5 \text{ m}) \quad (7)$$

Therefore, if the initialization is performed using information from an RSSI-outlier (RSSI below -58.75 dB or above -42.56 dB), as determined from the interpolated path-loss

curve in Fig. 3, the initial distance is constrained to 0.5 m and 20 m, respectively. Outliers can result in an initial distance estimation of several hundred meters due to the logarithmic decay in path loss, despite the operator being very close (0.5 m) - or can lead to initial distances much closer than 0.5 m, although being much further away. These distances are assumed to be realistic within our setup and are tuning parameters, as no operator is expected to be closer than 0.5 m to a power tool when they receive the first advertisement, and no one is expected to be further than 20 m from a tool when it is activated. Utilizing such outliers as the initial estimation can cause convergence of the filter to wrong estimates, due to the non-linearity of the measurement model [49]. Hence, a maximal initial distance of 20 m is assumed; the filter can subsequently adjust to greater distances if necessary, or converge to a closer distance if the operator is closer.

Recapped, whenever a tag detects its asset to be active, it starts advertising its state in a 7 s interval. The wearable, constantly scanning, detects the advertisements and starts a new instance of the embedded EKF algorithm based on the received RSSI values from the advertisements. Once the advertisements stop (i.e. the tag went back to inactive), the final distance estimate is transmitted to the server together with the start and stop time.

B. Asset-User-Tracking

As the wearables do not have a global view of all wearables-to-tags distances, a centralized asset-user tracking algorithm has been implemented to match any used asset with its corresponding user (i.e., the wearable).

After collecting distance estimations of all wearables with respect to the tags, the basic idea is to assign a user to each active period of an asset. At the beginning, the server has a list of all active periods of the sensor tags sorted by their start times. A single device can have multiple active periods and thus be present multiple times in this list. The algorithm starts with the tag that became active first (i.e., the first in the list). The user, respectively wearable device, nearest to the tag is assigned to this active period of the asset. Subsequently, the nearest user is then assigned to each additional active period of a device, provided that the user is not already using an asset. This problem can be formulated as the following optimization problem:

Given is a set of all users and assets (can be extracted from the information transmitted by the wearable devices):

I : set of all wearable devices (users) i

J : set of all sensor tags (assets) j

t : current time step

(8)

$d(i, j, t)$: estimated distance between i and j at time t

b_{jt} : state of the asset j at time t

with b_{jt} being 1 if the asset is active at time t and 0 otherwise.

The decision variables are the assignment of a user i to an asset j , namely a_{ijt} , as well as a trust level c_{ijt} belonging to

this assignment:

$$a_{ijt} = \begin{cases} 1 & \iff i \text{ is using } j \text{ at time } t \\ 0 & \text{otherwise} \end{cases} \quad (9)$$

$$c_{ijt} = \begin{cases} 1 & \iff \text{the assignment } a_{ijt} \text{ is likely correct} \\ 0 & \text{otherwise} \end{cases}$$

Therefore, the optimization goal is to assign the nearest operator-asset combination at each time step, and therefore providing the assignments a_{ijt} and the trust level classifier c_{ijt} .

$$\text{minimize} \quad \sum_i \sum_j \sum_t a_{ijt} \cdot d(i, j, t) \quad (10)$$

$$\text{subject to} \quad \sum_i a_{ijt} = \begin{cases} 1 & \iff b_{jt} = 1, \forall j, t \\ 0 & \iff b_{jt} = 0, \forall j, t \end{cases} \quad (11)$$

$$a_{ij(t+1)} = a_{ijt} \iff b_{j(t+1)} = b_{jt} \quad (12)$$

$$c_{ijt} = 1 \iff (a_{ijt} = 1) \wedge (|d(i, j, t) - d(k, j, t)| > 0.75 \text{ m}) \quad \forall k \in I \quad (13)$$

The optimization is subject to the constraint that each asset can only be used by exactly one user at any given time and that the asset must be active (Eq. (11)). Finally, the system is restricted to the extent that the operator cannot change during a continuous active time (session) of a device (Eq. (12)). Assignments a_{ijt} are provided with a trust level classifier, namely c_{ijt} , to account for residual EKF distance estimation errors. Whenever the estimated distance between the matched user and the next nearest user is less than 0.75 m (as described in Eq. (13) with \wedge being the logical conjunction operation), a classifier of 'UNSURE' is assigned to this matching. A classifier of 'SURE' means that the solution of the optimization problem matches the actual asset-user pairing with a high degree of certainty.

To solve the problem, Algorithm 1 is executed for each time step, starting from $t = 0$. In an initial step, inactive tools are unassigned ($\sum_i a_{ijt} = 0$, Eq. (11)) and the continuity constraint Eq. (12) is applied (Lines 4 to 7) in order to reduce the search space. Then, an exhaustive search is executed as in Line 9.

The exhaustive search iterates through the reduced sets I and J , evaluating the cost function of Eq. (10) and returning the assignment leading to the lowest cost value. In most cases, only a single asset is started or stopped simultaneously during a given time step, reducing J to a singleton, and the search to finding the nearest operator of the asset.

For the practical implementation of the system (Section III), the following limitations apply:

- To distinguish between two subsequent asset activities of an asset, there must be a minimum pause of 21 s to be considered as two activities (3 advertisements, 7 s each).
- With a classifier of 'UNSURE', there is an increased risk that the solution is incorrect, or multiple users have been working on the same tool. The distance of 0.75 m comes from the assumption that two users do generally not stand closer to each other.

V. EXPERIMENTAL SETUP

In order to evaluate the accuracy of the algorithms, an experimental setup was set up in the construction sector, where construction workers (our users) are to be matched to the power tools used (our assets).

A. Hardware setup

The SMARTTAG has been used as the sensor node for the experimental evaluation. It is a smart BLE beacon targeted for ultra-low power consumption and built for easy retrofit on existing power tools. The SMARTTAG is built around an nRF52810 BLE SoC from Nordic Semiconductor. The SoC integrates an ARM Cortex-M4F with BLE 5.3 connectivity, 192 kB Flash, and 24 kB RAM. Evaluating the measurements of the ultra-low power accelerometer IIS2DLPC from STMICROELECTRONICS, it advertises every 7 s the asset's current state: active working (*Usage* class), any other non-active working phase present during construction activity (*Transportation* class), and inactivity. A simple fast Fourier transform (FFT)-based approach was used in the first implementation [18], which only worked with one type of drill (Hilti TE 30-A36); then, a computational-heavy implementation using neural networks was implemented [50], followed by a MINIROCKET-based version [51], which can classify activity on a variety of power tools (drills, hammers, etc.). The MINIROCKET-based classification achieves an accuracy of 96.9% across 16 tested power tools of different manufacturers. The 7 s interval was defined in [51] as the optimum trade-off between update frequency and power consumption. Assuming a typical usage duration of power tools between 30 s and 120 min [52], [53], this corresponds to at least four measurements of RSSI values, which already provide enough informations for an initial distance estimation. Having a power consumption of only 15 μ W, its battery life is estimated to be more than three years on a 675 mWh battery.

As wearable device, the ECOTRACK [22] has been used. The wearable device is worn by each construction worker on the chest, which was found to be the most comfortable position during testing. However, the position can easily be adjusted if, for example, a smartwatch is used. The ECOTRACK consists of an nRF52833, a BLE-enabled Cortex-M4 from NORDIC SEMICONDUCTOR. It has been used to track the worker's condition using its SARA R510M8S global navigation satellite system (GNSS) and LTE-M module and an LSM6DSLTR inertial measurement unit (IMU). Achieving a power consumption of 16 mW while being connected over LTE-M and scanning for BLE advertisement, it is prepared to operate for a multiple weeks on a single battery charge of 10 800 mWh. Using an encrypted MQTT (MQTT) connection to the server, messages can be exchanged asynchronously by the ECOTRACK and the server.

The centralized server was implemented using AWS Lambdas, where a Lambda receives the data via MQTT and stores it in a database. New data then triggers a second Lambda, which solves the linear program from Section IV-B and makes the data available to the end user in a dashboard.

Algorithm 1 Iterative Asset-Operator Matching to find a_{ijt}

```

1: function MATCHING( $I, J, t, d, a_{0:t-1}, b_{0:t}$ )
2:    $a_{ijt} \leftarrow 0 \forall i \in I, j \in J$  ▷ Initialize solution for time step  $t$  with zero
3:   for all  $j \in J$  do ▷ Inactive assets are not assigned to an operator.
4:     if  $b_{it} = 0$  then
5:        $a_{ijt} \leftarrow 0 \forall i \in I$  ▷ Assets active in previous time step do not change operator.
6:     else if  $b_{it} = b_{i(t-1)} = 1$  then
7:        $a_{ijt} \leftarrow a_{ij(t-1)} \forall i \in I$  ▷ Assign newly activated assets to the correct operator
8:     else ▷ by searching through the solution space
9:       exhaustiveSearch()
10:    end if
11:  end for
12: end function

```

B. Measurement setup

To quantify the accuracy of the proposed system, tests were conducted both indoors and outdoors. During these tests, tags were mounted on various power tools (Hilti SFC 14-A, Hilti TE 30-A36, Hilti TE 706-AVR, Hilti SF 10W-A22), and a wearable was attached to the chest of each worker. During the indoor measurements, the exact position of all devices was recorded with the OPTITRACK system¹. The data obtained by the OPTITRACK is used as ground truth, especially for distance estimation. During all measurements, a NIKON Z6 II video camera was used to record the test and as a sanity check for correct asset-user tracking. The following measurement tests were performed indoors:

- 1) One worker on a power tool, one person standing close by with a distance of 0.5 m, 1 m, 2 m, 3 m respectively.
- 2) One worker on a power tool, two persons standing close by with distances of 0.5 m, 1 m, 2 m, 3 m each.
- 3) Two workers working on a power tool each, working at distances of 0.5 m, 1 m, 2 m, 3 m.
- 4) Two workers working on a power tool each, working at distances of 0.5 m, 1 m, 2 m, 3 m. One person standing close by with a distance of 0.5 m, 1 m, 2 m, 3 m.
- 5) Three workers working on a power tool each, working at distances of 0.5 m, 1 m, 2 m, 3 m.
- 6) Three workers working on a power tool each, working at distances of 2 m. After 2 min and 4 min, they swap the power tools with each other. These results are presented in Fig. 7

Each of those experiments was conducted for 3 min to 6 min. Data was collected with an advertising interval of 0.5 s; to replicate the 7-second interval, data was downsampled to match an advertisement interval of 7 s. In this way, a fourteen times larger 7-second dataset was obtained. The last experiment shows a dynamic use case, where workers change tools between them.

In a later step, the following measurement tests were performed outdoors:

- 1) One worker on a power tool, one person standing close by with a distance of 0.5 m, 1 m, 2 m, 3 m respectively.
- 2) Two workers on a power tool each, working at distances of 0.5 m, 1 m, 2 m, 3 m.

- 3) Three workers on a power tool each, working at distances of 0.5 m, 1 m, 2 m, 3 m.
- 4) Three workers on a power tool each, working at changing distances between each other.

The last experiment shows a dynamic use case in the outdoor environment, where the workers change their working distances with respect to each other.

Fig. 2 shows the outdoor experimental setup. The indoor setup was correspondingly the same.

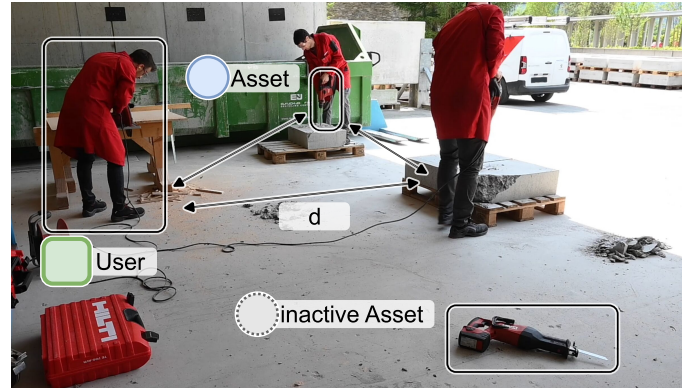


Fig. 2. Outdoor experimental setup. Three workers, each with their own asset, separated all by a distance d of 2 m

The power measurements were conducted using a KEYSIGHT N6705C with the N6781A module. The following measurements were taken:

- 1) Power consumption of the badge in scanning mode (i.e., only BLE scanning)
- 2) Power consumption of the badge during the calculation of the distance estimation algorithm (i.e., BLE off, central processing unit (CPU) computing at 64 MHz)
- 3) Power consumption of the badge transmitting values to the cloud (i.e., only LTE-M active)

The power consumption of the SMARTTAG has been reported and discussed in detail in [51].

VI. RESULTS

This section presents the measurements performed to fit the path-loss equation to our RSSI data. It determines the accuracy of the two algorithms explained in Section IV-A

¹<https://optitrack.com/>, 08.02.2024

and Section IV-B. In particular, the accuracy of the calculated distances of the EKF and cumulative average (CA) algorithms are compared to their ground truth. Afterwards, the results of the asset-to-user matching based on the aforementioned distance estimations are presented. Subsequently, each of the two implications is discussed, and the occurrence of the measurement errors is examined in more detail. Finally, the power consumption of the algorithm implemented on the wearable device is presented.

A. Path-loss fitting

Fig. 3 shows Eq. (1) fitted to all our measurements (55'097 RSSI values, $n = 1.011$, $x_0 = 1$ m, $RSSI(x_0) = -45.6$ dB, experimental setup as in Section V). These values are used in the EKF of the badge for estimating the distance between tag and badge.

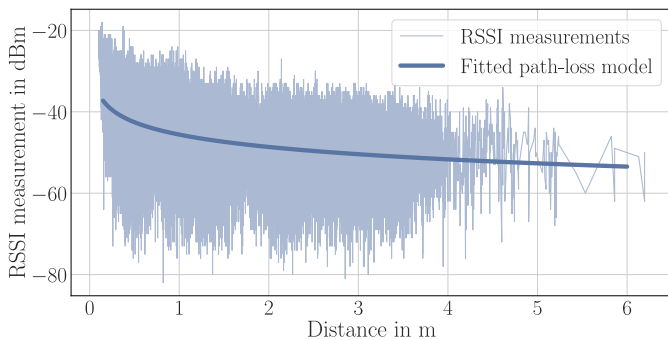


Fig. 3. RSSI measurements versus ground truth distance together with fitted path-loss equation (Eq. (1)). Does not include results of dynamic measurements.

The variance of all raw RSSI values with respect to the fitted path-loss curve is 48.92 dB^2 , and the standard deviation is 6.99 dB . It can be seen that individual RSSI readings at a distance of 6 m can also occur at a distance of less than 50 cm - the map is, therefore, no longer bijective due to the aforementioned imperfections. However, the trend of a logarithmic curve can still be recognized.

B. Distance estimation

In our experiments' scope, a total of 2338 distance estimates were made at different measurement distances. These estimates are used in the following and compared to their ground truth distance to evaluate the accuracy and precision of the estimates. The amount of estimations per ground truth distance vary, as can be seen in Fig. 4. As the distance between a user and its asset during the experiments was always below 0.5 m , 35.07% of all estimations were carried in the range between 0 m and 0.5 m . To investigate the accuracy of the distance estimation, all distances estimated by the badges were compared with their ground truth values recorded by the OPTITRACK system, and the estimation error was calculated. An overview of these results can be found in Table II.

The calculated estimation error is 0.49 m in median with a standard deviation of 1.63 m and a variance of 2.67 m^2 . These results, plotted as a histogram with associated interquartile

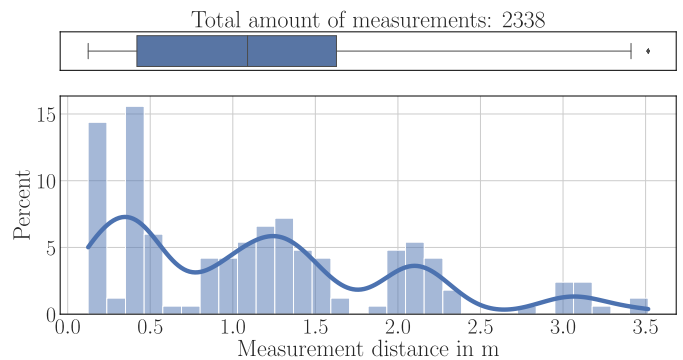


Fig. 4. Distribution of the 2338 performed measurements according to their ground truth distances. Does not include results of dynamic measurements.

TABLE II
STATISTICS OF THE DISTANCE ESTIMATION ALGORITHM

Quantity	Measure
2338	Total amount of estimated distances
0.49 m	Median Error
1.18 m	Mean Absolute Error
1.92 m	Root Mean Square Error
1.63 m	Standard Deviation
2.67 m^2	Variance
11.78 m	Maximum (Absolute) Error
0.00 m	Minimum (Absolute) Error

range (IQR) ($[0.12 \text{ m}, 1.37 \text{ m}]$) and whiskers in Fig. 5, show that 90.98% of all estimations (represented by whiskers) are within $[-1.76 \text{ m}, 3.24 \text{ m}]$. The breakdown of these estimation

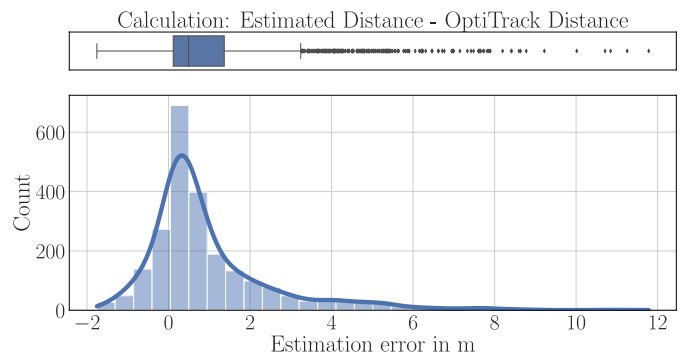


Fig. 5. Estimation error with respect to ground truth, evaluated over all 2338 estimations. Box-whisker plot highlighting the distribution of the values. Does not include results of dynamic measurements.

errors against their ground truth values, as shown in Fig. 6, shows that the ground truth distance influences the estimation error: The median error for all ground truth distances smaller than 1 m is 0.37 m . The estimations especially lie close together, with the variance being 0.34 m^2 . When the effective distance increases, the median slightly increases to 0.86 m for all distances higher than 1 m , and the variance grows to 4.25 m^2 .

This behavior can be explained by the fact that the logarithmic decay of the theoretical path-loss model (Eq. (1)) reacts much stronger to measurement inaccuracies and disturbances

of the RSSI the further the distance between the devices is. The distances between 2.5 m and 3 m contributed to only 1.80% of all estimations and were all recorded during a single experiment. They are, therefore, insufficient to draw statistical conclusions.

If these results are compared with [43], it is noticeable that the accuracy of our distance estimation is about 0.5 m higher, even though the same EKF is used. There may be several reasons for this, but mainly:

- A different path-loss model is used: while [43] uses a fit to the exponential function $h(x) = ae^{bx} + ce^{dx} - o$, here the model as shown in Eq. (1) is used. Due to the smaller number of parameters, our model is less dependent on the environment, thus adapting more accurately to changes in the environment.
- The distance between the asset and the user is almost constant in our model, while the distance between the node and the tag in [43] changes between 1 m and 5 m. Due to the exponential decay of the path-loss, measurement errors are bigger on larger distances.
- Different radio frontends were used ([43]: ESP32), the measurement accuracy of RSSI can therefore vary.

C. Asset - User Matching

The 2338 distance estimations led to 980 matches between worker and tool. 546 of those matches are done in the indoor setup, and 434 in the outdoor setup.

Following up on the trust classifier, the following evaluation classes are used to characterize our results:

True Positive 'SURE':

This is the class of all correct matches, and in which the algorithm had a confident sense during the assignment. The goal is to have as many results as possible in this classification.

False Negative 'UNSURE':

In this class are all results where the algorithm led to the correct result, but the matching was classified with little confidence. Possibilities for this are either that the distances between users were so small that it is difficult to judge which one used the asset; or a distance estimate that deviated from the actual distance.

True Negative 'UNSURE':

This class represents the matches with a wrong result, but where the trust was also low. This class is the analog of the previous one, but where the matching was wrong.

False Positive 'SURE':

The last class is the one that can be described as definitely false. The algorithm has made a matching here, which is wrong - but was quite sure that the matching is correct. These are the results that are to be minimized.

The reported results can be seen in Fig. 7 and demonstrate the algorithm's performance in both indoor and outdoor scenarios.

In the indoor environment, the algorithm achieved an overall accuracy of 89.7%, with the accuracy defined in Eq. (14)

$$A = \frac{C}{T} \quad (14)$$

where C is the number of correct matches and T is the total number of matches.

Notably, the majority of correct classifications were made with high confidence, as evidenced by the "Guessed correct and 'SURE'" category, giving a recall as per Eq. (15) of 70.8%.

$$R = \frac{C_{\text{sure}}}{C} \quad (15)$$

where C_{sure} is the number of correct matches with high trust level.

The precision, indicating the probability that when the algorithm assigns a trust level of 'SURE', the matching was correct as defined in Eq. (16), in the indoor setting was exceptionally high (98.6%). However, addressing the cases where the algorithm exhibited uncertainty is essential.

$$P = \frac{C_{\text{sure}}}{T_{\text{sure}}} \quad (16)$$

where T_{sure} is the total number of matches with high trust level.

In the "Guessed correct but trust level 'UNSURE'" category, there were 143 instances indoors, highlighting situations where the algorithm correctly identified the match but lacked confidence. Fig. 8 shows that a higher distance between the different workers generally resulted in a more reliable assignment between the worker and the tools.

In contrast, the outdoor scenario demonstrated an even higher overall accuracy of 98.6%. The algorithm exhibited a remarkable recall of 95.8% and perfect precision (100%) in correctly classifying matches with high confidence ("Guessed correct and 'SURE'"). This suggests the algorithm's robustness in outdoor environments, where there are potentially fewer collisions and reflections, and therefore, a more deterministic path loss occurs.

The absence of "Guessed wrong and 'SURE'" instances in the outdoor environment is promising, indicating that the algorithm, when wrong, tends to express uncertainty. This is a crucial characteristic, as it prevents the algorithm from confidently producing incorrect results.

It should also be noted that a similarly high precision of 98.9% was achieved in the dynamic scenarios, with the recall even increasing to 92.8%. It can therefore be concluded that the detection of individual matchings works reliably even under more dynamic constraints. The reasons for the higher values could be the different dynamics between the correct matching and all other possible matchings: while there is relatively little movement between the user and his asset, the relative change in distance between a user and the other assets is greater - resulting in a more variable and bigger distance estimation.

In conclusion, while the algorithm showcases strong performance in both indoor and outdoor settings, addressing instances of uncertainty, especially in indoor scenarios, can be a focus for improvement. These findings contribute valuable insights to the ongoing development and optimization of asset-matching algorithms in various environmental conditions.

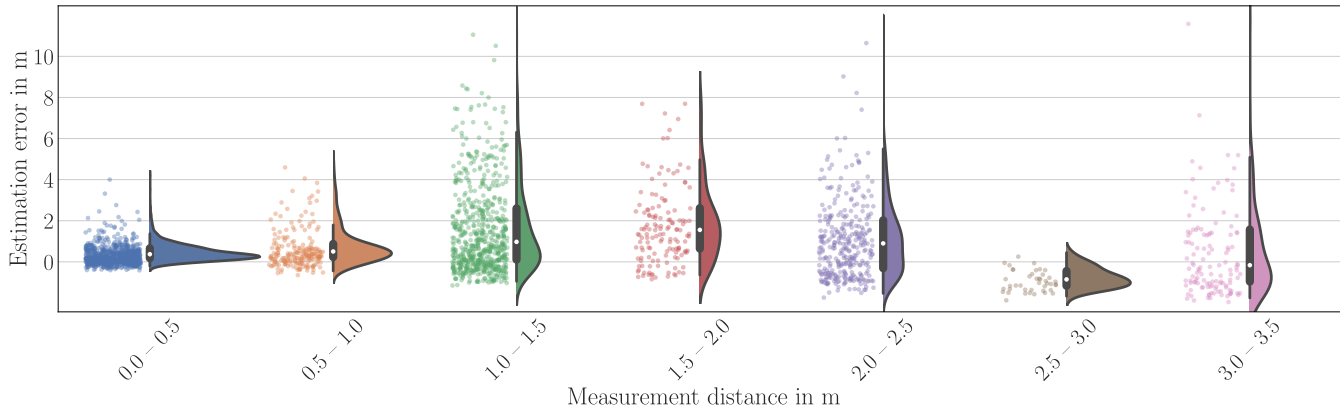


Fig. 6. Distribution of estimation errors against their ground truth distances. The errors of each distance bin are represented as swarm and as half-violin with IQR and Whiskers. Does not include results of dynamic measurements.

Matching	(a) Indoor		(b) Outdoor	
	Sure	Unsure	Sure	Unsure
Correct	347 64%	143 26%	410 94%	18 4%
Wrong	5 1%	51 9%	0 0%	6 1%

Fig. 7. Confusion matrix of the (a) indoor and (b) outdoor experiments. Results reported in absolute numbers of measurements, dark blue color means many results, white means few.

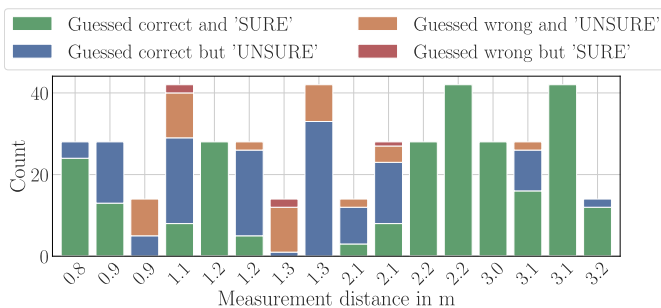


Fig. 8. Results in the indoor setup, divided up according the ground truth distance between asset and user. Does not include results of dynamic measurements.

D. Power measurements on the wearable device

Table III shows a breakdown of the power consumption of the basic functionality and algorithms implemented on the wearable device. A working day of 8 hours was assumed, during which 20 different devices were active and recognized for 1.5 hours each. This corresponds to 15k advertisements that have to be processed by the wearable device per day.

The largest energy consumer on the wearable device is the constant scanning for advertisements, with 0.31 Wh. This is followed by the LTE-M module, which is in cyclic idle/active mode most of the time ($DRX = 1.28$ s, no eDRX) and active for less than 10 s per day in order to transmit the collected data to the server. Compared to this power consumption, the

TABLE III
POWER CONSUMPTION BREAKDOWN OF THE WEARABLE DEVICE (ECOTRACK) DURING DIFFERENT ACTIVITIES. SYSTEM VOLTAGE 3.8 V

Part	Power state	Power consumption	Duration per day	Energy per day
Baseline	switched-off	296.00 nW	16 h	4.7 μ Wh
MCU	BLE scan.	38.38 mW	8 h	0.31 Wh
	updating EKF	21.70 mW	1.37 s	8.2 μ Wh
LTE-M	transmitting	456.00 mW	< 10 s	< 1.3 mWh
	idle connected	9.12 mW	8 h	73 mWh
	deep sleep	266.00 μ W	16 h	4.3 mWh
Average per day		16.06 mW		0.39 Wh

energy consumption of the EKF is small, with 8.2 μ Wh. One iteration of the EKF requires 5698 cycles on the ECOTRACK, corresponding to an active time of 1.37 s for the 15k daily advertisements.

In total, the wearable device consumes an average power of 16.06 mW. With the available 10 800 mWh battery, this results in a runtime of 28 days; enough to be charged only once every four weeks. This is particularly important, as it causes no substantial overhead to charge the devices.

VII. CONCLUSION

This study introduced a novel approach enabling asset-user matching in industrial environments using Bluetooth Low Energy (BLE)-enabled low-power IoT devices. The system comprises BLE-based tags equipped with accelerometers, wearable devices with internet access, and two algorithms:

- i) A distance estimation algorithm based on Extended Kalman Filter (EKF) to enhance the accuracy of distance estimations from RSSI measurements. Despite challenges such as noise and measurement errors, the system achieved a median distance estimation error of 0.49 m in the range of interest.
- ii) A cloud-based algorithm for asset-to-user matching that effectively matched assets with their users, achieving an

accuracy of 87.7% in indoor environments and 98.6% in outdoor environments.

Furthermore, the system was validated through extensive indoor and outdoor experiments in real construction settings. This work proved that it is feasible to provide asset-user matches in real-world scenarios underscoring its utility for enhanced operational efficiency and safety. Additionally, the proposed approach optimizes power consumption across all components. The BLE tags can operate for years on a single coin-cell battery. By reducing the data transmission load to the cloud server, the wearable devices are able to extend their operational lifetime to approximately 28 days on a 10 800 mWh battery. This aspect is crucial for widespread adoption in industrial environments where maintenance overhead must be minimized. Future works could focus on extending the testing to different environments with a sensitivity analysis on the algorithm's tuning parameters to validate its robustness and generalization capabilities.

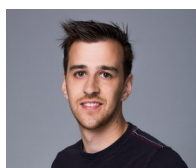
REFERENCES

- [1] B. Bajic, A. Rikalovic, N. Suzic, and V. Piuri, "Industry 4.0 implementation challenges and opportunities: a managerial perspective," *IEEE Systems Journal*, vol. 15, no. 1, pp. 546–559, 2021. [Online]. Available: <http://dx.doi.org/10.1109/JSYST.2020.3023041>
- [2] A. Rikalovic, N. Suzic, B. Bajic, and V. Piuri, "Industry 4.0 implementation challenges and opportunities: a technological perspective," *IEEE Systems Journal*, vol. 16, no. 2, pp. 2797–2810, 2022. [Online]. Available: <http://dx.doi.org/10.1109/JSYST.2021.3101673>
- [3] A. Zanella, N. Bui, A. Castellani, L. Vangelista, and M. Zorzi, "Internet of things for smart cities," *IEEE Internet of Things Journal*, vol. 1, no. 1, pp. 22–32, 2014. [Online]. Available: <http://dx.doi.org/10.1109/JIOT.2014.2306328>
- [4] N. N. Misra, Y. Dixit, A. Al-Mallahi, M. S. Bhullar, R. Upadhyay, and A. Martynenko, "Iot, big data, and artificial intelligence in agriculture and food industry," *IEEE Internet of Things Journal*, vol. 9, no. 9, pp. 6305–6324, 2022. [Online]. Available: <http://dx.doi.org/10.1109/JIOT.2020.2998584>
- [5] C. J. Turner, J. Oyekan, L. Stergioulas, and D. Griffin, "Utilizing industry 4.0 on the construction site: Challenges and opportunities," *IEEE Transactions on Industrial Informatics*, vol. 17, no. 2, pp. 746–756, 2021. [Online]. Available: <http://dx.doi.org/10.1109/TII.2020.3002197>
- [6] S. Demirkesen and A. Tezel, "Investigating major challenges for industry 4.0 adoption among construction companies," *Engineering, Construction and Architectural Management*, vol. 29, no. 3, pp. 1470–1503, 2021. [Online]. Available: <http://dx.doi.org/10.1108/ECAM-12-2020-1059>
- [7] A. Alvand, S. M. Mirhosseini, M. Ehsanifar, E. Zeighami, and A. Mohammadi, "Identification and assessment of risk in construction projects using the integrated fmea-swara-waspas model under fuzzy environment: a case study of a construction project in iran," *International Journal of Construction Management*, vol. 23, no. 3, pp. 392–404, 2021. [Online]. Available: <http://dx.doi.org/10.1080/15623599.2021.1877875>
- [8] B. Huffstutler, 11 2023, last access: 15.02.2024. [Online]. Available: <https://news.ararental.org/hilti-adds-more-than-50000-tool-tags-to-trackunit-platform>
- [9] B. Sherafat, C. R. Ahn, R. Akhavian, A. H. Behzadan, M. Golparvar-Fard, H. Kim, Y.-C. Lee, A. Rashidi, and E. R. Azar, "Automated methods for activity recognition of construction workers and equipment: State-of-the-art review," *Journal of Construction Engineering and Management*, vol. 146, no. 6, p. 19, 2020. [Online]. Available: [http://dx.doi.org/10.1061/\(ASCE\)CO.1943-7862.0001843](http://dx.doi.org/10.1061/(ASCE)CO.1943-7862.0001843)
- [10] S. de Fatima F. Barbosa and G. T. M. D. Sasso, *Patient Safety: Opportunities and Risks of Health IT Applications, Methods and Devices*, ser. Health Informatics. Springer International Publishing, 2022, pp. 357–374. [Online]. Available: http://dx.doi.org/10.1007/978-3-030-91237-6_24
- [11] A. Luschi, G. Ghisalbetti, G. L. Daino, V. Mezzatesta, and E. Iadanza, *OHIO: Integrating IoT Technologies for Enhanced Clinical Engineering and Dynamic Tracking of Medical Equipment*, ser. IFMBE Proceedings. Springer Nature Switzerland, 2024, pp. 169–177. [Online]. Available: http://dx.doi.org/10.1007/978-3-031-61628-0_19
- [12] Z. Zhao, P. Lin, L. Shen, M. Zhang, and G. Q. Huang, "Iot edge computing-enabled collaborative tracking system for manufacturing resources in industrial park," *Advanced Engineering Informatics*, vol. 43, p. 101044, 2020. [Online]. Available: <http://dx.doi.org/10.1016/j.aei.2020.101044>
- [13] R. Edirisinghe, "Digital skin of the construction site," *Engineering, Construction and Architectural Management*, vol. 26, no. 2, pp. 184–223, 2018. [Online]. Available: <http://dx.doi.org/10.1108/ECAM-04-2017-0066>
- [14] K. Khurshid, A. Danish, M. U. Salim, M. Bayram, T. Ozbakkaloglu, and M. A. Mosaberpanah, "An in-depth survey demystifying the internet of things (iot) in the construction industry: Unfolding new dimensions," *Sustainability*, vol. 15, no. 2, p. 1275, 2023. [Online]. Available: <http://dx.doi.org/10.3390/su15021275>
- [15] R. Ranjithapriya, D. S. Arulsevan, and C. institute of technology, "Study on factors affecting equipment management and its effect on productivity in building construction," *International Journal of Engineering Research and*, vol. V9, no. 04, p. 8, 2020. [Online]. Available: <http://dx.doi.org/10.17577/IJERTV9IS040176>
- [16] H. Li, G. Chan, J. K. W. Wong, and M. Skitmore, "Real-time locating systems applications in construction," *Automation in Construction*, vol. 63, pp. 37–47, 2016. [Online]. Available: <http://dx.doi.org/10.1016/j.autcon.2015.12.001>
- [17] A. Mackey, P. Spachos, L. Song, and K. N. Plataniotis, "Improving ble beacon proximity estimation accuracy through bayesian filtering," *IEEE Internet of Things Journal*, vol. 7, no. 4, pp. 3160–3169, 2020. [Online]. Available: <http://dx.doi.org/10.1109/JIOT.2020.2965583>
- [18] M. Giordano, R. Fischer, M. Crabolu, G. Bellusci, and M. Magno, "Smarttag: An ultra low power asset tracking and usage analysis iot device with embedded ml capabilities," in *2021 IEEE Sensors Applications Symposium (SAS)*, 8 2021, p. 6. [Online]. Available: <http://dx.doi.org/10.1109/SAS51076.2021.9530182>
- [19] S. Krishnan and R. X. M. Santos, *Real-Time Asset Tracking for Smart Manufacturing*, ser. Intelligent Systems Reference Library. Springer International Publishing, 2021, ch. 2, pp. 25–53. [Online]. Available: http://dx.doi.org/10.1007/978-3-030-67270-6_2
- [20] M. Magno, L. Sigrist, A. Gomez, L. Cavigelli, A. Libri, E. Popovici, and L. Benini, "Smarteg: an autonomous wireless sensor node for high accuracy accelerometer-based monitoring," *Sensors*, vol. 19, no. 12, p. 2747, 2019. [Online]. Available: <http://dx.doi.org/10.3390/s19122747>
- [21] F. E. Murphy, M. Magno, P. Whelan, and E. P. Vici, "b+wsn: Smart beehive for agriculture, environmental, and honey bee health monitoring - preliminary results and analysis," in *2015 IEEE Sensors Applications Symposium (SAS)*, 4 2015, p. nil. [Online]. Available: <http://dx.doi.org/10.1109/SAS.2015.7133587>
- [22] M. Giordano, S. Cortesi, P.-V. Mekikis, M. Crabolu, G. Bellusci, and M. Magno, "Energy-aware adaptive sampling for self-sustainability in resource-constrained iot devices," in *Proceedings of the 11th International Workshop on Energy Harvesting & Energy-Neutral Sensing Systems*, 11 2023, pp. 65–71. [Online]. Available: <http://dx.doi.org/10.1145/3628353.3628545>
- [23] P. M. Goodrum, M. A. McLaren, and A. Durfee, "The application of active radio frequency identification technology for tool tracking on construction job sites," *Automation in Construction*, vol. 15, no. 3, pp. 292–302, 2006. [Online]. Available: <http://dx.doi.org/10.1016/j.autcon.2005.06.004>
- [24] J. D. Goedert, E. T. Foster, J. Jewell, and J. Bartek, "Automated tool tracking on the construction site," *International Journal of Construction Education and Research*, vol. 5, no. 1, pp. 12–23, 2009. [Online]. Available: <http://dx.doi.org/10.1080/15578770902717535>
- [25] S.-G. Kwon, O.-J. Kwon, K.-R. Kwon, and S.-H. Lee, "Uwb and mems imu integrated positioning algorithm for a work-tool tracking system," *Applied Sciences*, vol. 11, no. 19, p. 8826, 2021. [Online]. Available: <http://dx.doi.org/10.3390/app11198826>
- [26] F. Zafari, A. Gkelias, and K. K. Leung, "A survey of indoor localization systems and technologies," *IEEE Communications Surveys & Tutorials*, vol. 21, no. 3, pp. 2568–2599, 2019. [Online]. Available: <http://dx.doi.org/10.1109/COMST.2019.2911558>
- [27] L. Fluoratoru, S. Wehrli, M. Magno, and D. Niculescu, "On the energy consumption and ranging accuracy of ultra-wideband physical interfaces," in *GLOBECOM 2020 - 2020 IEEE Global Communications Conference*, 12 2020, p. 7. [Online]. Available: <http://dx.doi.org/10.1109/GLOBECOM42002.2020.9347984>
- [28] S. Koenig, M. T. Schmidt, and C. Hoene, "Multipath mitigation for indoor localization based on iee 802.11 time-of-flight measurements," in *2011 IEEE International Symposium on a World of Wireless, Mobile*

- and Multimedia Networks*. Lucca, Italy: IEEE, 6 2011, p. 8. [Online]. Available: <http://dx.doi.org/10.1109/WoWMoM.2011.5986392>
- [29] S. Cortesi, C. Vogt, and M. Magno, "Comparison between an rssi- and an mcpd-based ble indoor localization system," *Computers*, vol. 12, no. 3, p. 59, 2023. [Online]. Available: <http://dx.doi.org/10.3390/computers12030059>
- [30] H. Friis, "A note on a simple transmission formula," *Proceedings of the IRE*, vol. 34, no. 5, pp. 254–256, 1946. [Online]. Available: <http://dx.doi.org/10.1109/JRPROC.1946.234568>
- [31] Y.-C. Pu and P.-C. You, "Indoor positioning system based on ble location fingerprinting with classification approach," *Applied Mathematical Modelling*, vol. 62, pp. 654–663, 2018. [Online]. Available: <https://doi.org/10.1016/j.apm.2018.06.031>
- [32] A. Balakrishnan, K. Ramana, K. Nanmaran, M. Ramachandran, V. Bhaskar, and S. Kallam, "Rssi based localization and tracking in a spatial network system using wireless sensor networks," *Wireless Personal Communications*, vol. 123, no. 1, pp. 879–915, 2021. [Online]. Available: <http://dx.doi.org/10.1007/s11277-021-09161-0>
- [33] A. Castiglione, M. Umer, S. Sadiq, M. S. Obaidat, and P. Vijayakumar, "The role of internet of things to control the outbreak of covid-19 pandemic," *IEEE Internet of Things Journal*, vol. 8, no. 21, pp. 16 072–16 082, 2021. [Online]. Available: <http://dx.doi.org/10.1109/JIOT.2021.3070306>
- [34] N. Pathak, P. K. Deb, A. Mukherjee, and S. Misra, "Tot-to-the-rescue: a survey of iot solutions for covid-19-like pandemics," *IEEE Internet of Things Journal*, vol. 8, no. 17, pp. 13 145–13 164, 2021. [Online]. Available: <http://dx.doi.org/10.1109/JIOT.2021.3082838>
- [35] S. Kumar, V. Gautam, A. Kumar, and P. Kumari, "Social distancing using bluetooth low energy to prevent the spread of covid-19," in *2021 11th International Conference on Cloud Computing, Data Science & Engineering (Confluence)*, 1 2021, p. 5. [Online]. Available: <http://dx.doi.org/10.1109/Confluence51648.2021.9377096>
- [36] H. Agarwal, N. Sanghvi, V. Roy, and K. Kitani, "Deepble: Generalizing rssi-based localization across different devices," 2021. [Online]. Available: <https://arxiv.org/abs/2103.00252>
- [37] H. Schulten, M. Kuhn, R. Heyn, G. Dumphart, F. Trosch, and A. Wittneben, "On the crucial impact of antennas and diversity on ble rssi-based indoor localization," in *2019 IEEE 89th Vehicular Technology Conference (VTC2019-Spring)*, 4 2019, p. 6. [Online]. Available: <http://dx.doi.org/10.1109/VTCSpring.2019.8746717>
- [38] T. He, J. Tan, W. Zhuo, M. Printz, and S.-H. G. Chan, "Tackling multipath and biased training data for imu-assisted ble proximity detection," in *IEEE INFOCOM 2022 - IEEE Conference on Computer Communications*, 5 2022, p. 10. [Online]. Available: <http://dx.doi.org/10.1109/INFOCOM48880.2022.9796716>
- [39] S. Naghdi and K. O'Keefe, "Trilateration with ble rssi accounting for pathloss due to human obstacles," in *2019 International Conference on Indoor Positioning and Indoor Navigation (IPIN)*, 9 2019, p. 8. [Online]. Available: <http://dx.doi.org/10.1109/IPIN.2019.8911816>
- [40] A. Goldsmith, *Wireless Communication*. Cambridge University Press, 2005. [Online]. Available: <https://doi.org/10.1017/CBO9780511841224>
- [41] S.-H. Lee, I.-K. Lim, and J.-K. Lee, "Method for improving indoor positioning accuracy using extended kalman filter," *Mobile Information Systems*, vol. 2016, pp. 1–15, 2016. [Online]. Available: <http://dx.doi.org/10.1155/2016/2369103>
- [42] M. A. Qathrady and A. Helmy, "Improving ble distance estimation and classification using tx power and machine learning," in *Proceedings of the 20th ACM International Conference on Modelling, Analysis and Simulation of Wireless and Mobile Systems*. Miami Florida, USA: ACM, 11 2017, p. 5. [Online]. Available: <http://dx.doi.org/10.1145/3127540.3127577>
- [43] J. M. G. de Gabriel, J. A. Fernández-Madrugal, A. López-Arquillos, and J. C. Rubio-Romero, "Monitoring harness use in construction with ble beacons," *Measurement*, vol. 131, pp. 329–340, 2019. [Online]. Available: <http://dx.doi.org/10.1016/j.measurement.2018.07.093>
- [44] S. Debnath and K. O'Keefe, "Proximity estimation with ble rssi and uwb range using machine learning algorithm," in *2023 13th International Conference on Indoor Positioning and Indoor Navigation (IPIN)*, 9 2023, p. 6. [Online]. Available: <http://dx.doi.org/10.1109/IPIN57070.2023.10332225>
- [45] I. V. Stelzer, J. Kager, and C. Herwig, *Comparison of Particle Filter and Extended Kalman Filter Algorithms for Monitoring of Bioprocesses*, ser. Computer Aided Chemical Engineering. Elsevier, 2017, pp. 1483–1488. [Online]. Available: <http://dx.doi.org/10.1016/B978-0-444-63965-3.50249-X>
- [46] J.-A. Fernandez-Madrugal and J. L. B. Claraco, *Simultaneous Localization and Mapping for Mobile Robots: Introduction and Methods*, 1st ed. USA: IGI Global, 2012.
- [47] M. S. Grewal and A. P. Andrews, *Kalman Filtering: Theory and Practice Using MATLAB*. John Wiley & Sons, Ltd, 2008. [Online]. Available: <https://onlinelibrary.wiley.com/doi/abs/10.1002/9780470377819.ch4>
- [48] K. Reif, S. Gunther, E. Yaz, and R. Unbehauen, "Stochastic stability of the discrete-time extended kalman filter," *IEEE Transactions on Automatic Control*, vol. 44, no. 4, pp. 714–728, 1999. [Online]. Available: <http://dx.doi.org/10.1109/9.754809>
- [49] M. Boutayeb, H. Rafaralahy, and M. Darouach, "Convergence analysis of the extended kalman filter used as an observer for nonlinear deterministic discrete-time systems," *IEEE Transactions on Automatic Control*, vol. 42, no. 4, pp. 581–586, 1997. [Online]. Available: <http://dx.doi.org/10.1109/9.566674>
- [50] M. Giordano, N. Baumann, M. Crabolu, R. Fischer, G. Bellusci, and M. Magno, "Design and performance evaluation of an ultralow-power smart iot device with embedded tinyml for asset activity monitoring," *IEEE Transactions on Instrumentation and Measurement*, vol. 71, pp. 1–11, 2022. [Online]. Available: <http://dx.doi.org/10.1109/TIM.2022.3165816>
- [51] M. Giordano, S. Cortesi, M. Crabolu, L. Pedrollo, G. Bellusci, T. Bendinelli, E. Türetken, A. Dunbar, and M. Magno, "Optimizing iot-based asset and utilization tracking: Efficient activity classification with minirocket on resource-constrained devices," 2023. [Online]. Available: <https://arxiv.org/abs/2310.14758>
- [52] M. Vergara, J.-L. Sancho, P. Rodríguez, and A. Pérez-González, "Hand-transmitted vibration in power tools: Accomplishment of standards and users' perception," *International Journal of Industrial Ergonomics*, vol. 38, no. 9–10, pp. 652–660, 2008. [Online]. Available: <http://dx.doi.org/10.1016/j.ergon.2007.10.014>
- [53] D. J. Edwards and G. D. Holt, "Hand-arm vibration exposure from construction tools: Results of a field study," *Construction Management and Economics*, vol. 24, no. 2, pp. 209–217, 2006. [Online]. Available: <http://dx.doi.org/10.1080/01446190500310643>



Silvano Cortesi (GS'22) received the B. Sc. and the M.Sc. degree in electronics engineering and information technology from ETH Zürich, Zürich, Switzerland in 2020 and 2021, respectively. He is currently pursuing the Ph.D. degree with the Center for Project-Based Learning at ETH Zürich, Zürich, Switzerland. His research work focuses on indoor localization, ultra-low power and self-sustainable IoT, wireless sensor networks and energy harvesting.



Michele Crabolu is an expert in biomedical embedded wearable technologies, sensor fusion and TinyML algorithms with a PhD in bioengineering and robotics from University of Genoa, Genoa, Italy, and more than ten clinical validation studies on wearable technologies. In 2021 he received a postgraduate diploma in Machine Learning and Artificial Intelligence from Columbia University. At the time of writing, he is technical program manager of the Corporate Research and Technology at Hilti Corporation. Before joining Hilti, he has worked for

Xsens Technologies as Lead Engineer leading the research on sensor fusion and motion capture subjects.



Prodromos-Vasileios Mekikis works as a Researcher at the Corporate Research and Technology unit of the Hilti Group. At Hilti, he is engaged in exploring innovative solutions for enhanced productivity, safety, and sustainability in the construction industry through the integration of cutting-edge IoT technologies and data-driven insights. In 2020, he was awarded a Marie Skłodowska-Curie Postdoctoral fellowship for his research on UAV networks. He got his PhD from the Technical University of Catalonia (UPC) in 2017. He also holds an Electrical

and Computer Engineering degree (2010) and an M.Sc. in System-on-Chip design (2012) from Aristotle University of Thessaloniki (AUTH) and Royal Institute of Technology (KTH), respectively. His main research interests include connectivity in massive IoT networks, UAV-based networking, wireless power transfer, embedded systems design, and network function virtualization.



Giovanni Bellusci has broad R&D industry experience in diverse technology domains including IoT, Machine Learning, Robotics, Sensing Technologies, and Sensor Fusion algorithms. He is currently Head of Robotics & Mechatronics at Hilti Corporation, a global supplier of tools and services for the construction industry. Before joining Hilti, he was the Director of Technology & CTO at Xsens Technologies, a leading innovator in motion capture and position tracking solutions for applications in Industrial, Robotics, Wearables, and Health. He holds a PhD

Degree in Electrical Engineering from Delft University of Technology, the Netherlands, and an Executive MBA with Distinction from London Business School, UK.



Christian Vogt (M'20) received the M.Sc. degree and the PhD in electrical engineering and information technology from ETH Zürich, Zürich, Switzerland, in 2013 and 2017, respectively. He is currently a post-doctoral researcher and lecturer at ETH Zürich, Zürich, Switzerland. His research work focuses on signal processing for low power applications, including field programmable gate arrays (FPGAs), IoT, wearables and autonomous unmanned vehicles.



Michele Magno (SM'13) is currently a Senior Scientist at ETH Zürich, Switzerland, at the Department of Information Technology and Electrical Engineering (D-ITET). Since 2020, he is leading the D-ITET center for project-based learning at ETH. He received his master's and Ph.D. degrees in electronic engineering from the University of Bologna, Italy, in 2004 and 2010, respectively. He is working in ETH since 2013 and has become a visiting lecturer or professor at several universities, namely the University of Nice Sophia, France, Enssat Lannion, France,

University of Bologna and Mid University Sweden, where currently is a full visiting professor at the electrical engineering department. His current research interests include smart sensing, low-power machine learning, wireless sensor networks, wearable devices, energy harvesting, low-power management techniques, and extension of the lifetime of batteries-operating devices. He has authored more than 220 papers in international journals and conferences. He is a senior IEEE member and an ACM member. Some of his publications were awarded as best papers awards at IEEE conferences. He also received awards for industrial projects or patents.